

Chiral nickel(II) and palladium(II) catalysts bearing strong electron-withdrawing fluorine groups: synthesis, characterization and their application in catalytic polymerization for ethylene and styrene

Jianchao Yuan*, Jie Zhao, Fengying Song, Weibing Xu, Yanqiong Mu, Jingjing Chen and Zhenghua Zhang



A series of new chiral and achiral nickel(II) and palladium(II) complexes, {bis[*N,N'*-(2,6-diethyl-4-naphthylphenyl)imino]-1,2-dimethylethane}dibromonickel **3a**, {bis[*N,N'*-(4-fluoro-2-methyl-6-*sec*-phenethylphenyl)imino]-1,2-dimethylethane}dibromonickel *rac*-(*RS*)-**3b**, {bis[*N,N'*-(4-fluoro-6-*sec*-phenethylphenyl)imino]-1,2-dimethylethane}dibromonickel *rac*-(*RR/SS*)-**3c** and {bis[*N,N'*-(4-fluoro-6-*sec*-phenethylphenyl)imino]-1,2-dimethylethane}dichloropalladium *rac*-(*RR/SS*)-**3d** were successfully synthesized and characterized. The molecular structures of representative ligand *rac*-(*RS*)-**2b**, nickel complex **3a**, *rac*-(*RR/SS*)-**3c** and palladium complex *rac*-(*RR/SS*)-**3d** were determined by X-ray crystallography. The structures of complexes **3a** and *rac*-(*RR/SS*)-**3c** have pseudo-tetrahedral geometry about the nickel center, showing C_2 molecular symmetry. However, the structure of palladium complex *rac*-(*RR/SS*)-**3d** has pseudo-square planar geometry about the palladium center, showing C_2 molecular symmetry. Complex **3e** {bis[*N,N'*-(2,6-dimethylphenyl)imino]-1,2-dimethylethane}dibromonickel was also synthesized for comparison. Nickel complex *rac*-(*RS*)-**3b** bearing strong electron-withdrawing fluorine group in the *para*-aryl position and a chiral *sec*-phenethyl group in the *ortho*-aryl position of the ligand (one methyl group in the *ortho*-aryl position) displays the highest catalytic activity for ethylene and styrene polymerization, and produced highly branched polyethylene and syndiotactic-rich polystyrene. However, palladium complex *rac*-(*RR/SS*)-**3d** shows low catalytic activity for ethylene and styrene polymerization due to the poor leaving group, Cl, attached to palladium and the unfavorable molecular structure. Copyright © 2014 John Wiley & Sons, Ltd.

Additional supporting information may be found in the online version of this article at the publisher's web-site.

Keywords: chiral Ni(II)/Pd(II) complexes; chiral α -diimine ligand; crystal structure; *sec*-phenethyl substituent; branched polyethylene; syndiotactic polystyrene

Introduction

An important frontier in the field of polymer synthesis is to develop new methods for the synthesis of polyolefins of defined molecular weight, stereochemistry and consistent composition. In contrast to metallocene catalysts based on early transition metals,^[1–4] Ni(II) and Pd(II) catalysts discovered by Brookhart and co-workers could produce branched polyethylene with different concentrations and individual length of branches, exclusively from the ethylene monomer and accommodated even polar monomers.^[5–19] However, they generally produce amorphous, atactic polymers.^[17] Recently, Coates and co-workers proposed a new Brookhart type catalyst for olefin polymerization which bears a new class of chiral anilines and their incorporation into α -diimine Ni(II) catalysts that exhibit stereoselectivity in α -olefin polymerization.^[20,21] However, Ni(II) or Pd(II) complexes bearing strong electron-withdrawing fluorine groups has yet to be studied.

Recently, we reported the 'chain walking polymerization' of ethylene using chiral^[13,22,23] or achiral^[11,12,24,25] α -diimine Ni(II) complexes. In this work, we report the synthesis and characterization

of a series of new chiral nickel and palladium complexes of types [NiBr₂(Ar-DAB)] and [PdCl₂(Ar-DAB)] (Ar-DAB = *N,N'*-diaryl-1,4-diaza-1,3-butadiene) bearing strong electron-withdrawing fluorine and bulky chiral *sec*-phenethyl groups in different aryl positions in the ligand, in order to study the influence of metal (Ni and Pd), chiral/achiral groups, electron-withdrawing fluorine groups, steric effects and polymerization temperature on catalyst activity, microstructure of polyethylene and, in particular, on the stereoregular structure of polystyrene.

* Correspondence to: Jianchao Yuan, Key Laboratory of Eco-Environment-Related Polymer Materials of Ministry of Education, Key Laboratory of Polymer Materials of Gansu Province, College of Chemistry and Chemical Engineering, Northwest Normal University, Lanzhou 730070, China. E-mail: jianchaoyuan@nwnu.edu.cn

Key Laboratory of Eco-Environment-Related Polymer Materials of Ministry of Education, Key Laboratory of Polymer Materials of Gansu Province, College of Chemistry and Chemical Engineering, Northwest Normal University, Lanzhou 730070, China

Experimental

General Considerations and Materials

All manipulations involving air and/or moisture-sensitive compounds were carried out with standard Schlenk techniques under nitrogen. Methylene chloride and *o*-dichlorobenzene were pre-dried with 4 Å molecular sieves and distilled from CaH₂ under dry nitrogen. Toluene, diethyl ether and 1,2-dimethoxyethane (DME) were distilled from sodium/benzophenone under an N₂ atmosphere. Anhydrous NiBr₂ (99%), 1-naphthylboronic acid (97%), trifluoromethanesulfonic acid (99%), Pd(OAc)₂ and diethylaluminum chloride (DEAC, 0.9 M solution in toluene) were obtained from Acros. 2,3-Butanedione (98%), 2,6-diethylaniline (98%), 4-fluoroaniline (98%) and 4-fluoro-2-methylaniline (98%) were purchased from Alfa Aesar and used without further purification. [NiBr₂(DME)] was synthesized according to the literature.^[26]

NMR spectra were recorded at 400 (¹H) and 100 (¹³C) MHz, respectively, on a Varian Mercury plus-400 instrument with TMS as internal standard. FT-IR spectra were recorded on a Digilab Merlin FTS 3000 FT-IR spectrophotometer in KBr pellets. The molecular weights and molecular weight distributions (*M_w*/*M_n*) of the polymers were determined by gel permeation chromatography–size exclusion chromatography (GPC-SEC) via a Waters Alliance GPCV2000 chromatograph and polystyrene was used as the standard, using 1,2,4-trichlorobenzene as eluent, at a flow rate of 1.0 ml min⁻¹ and operated at 140°C. The elemental content of samples was determined by elemental analyzer (Vaiio-EL106, Germany).

Synthesis of 4-bromo-2,6-diethylaniline

Acetic acid (2 ml) was added to a stirred solution of 2,6-diethylaniline (0.75 g, 5 mmol) in CH₂Cl₂. The solution was stirred for 30 min. After the solution was cooled to 5°C in an ice bath, Br₂ (0.96 g, 6.0 mmol) in 5 ml CH₂Cl₂ was slowly added to the stirred solution. The mixture was stirred for 6 h and neutralized by 10% saturated aqueous sodium hydroxide solution. The mixture was extracted three times with 50 ml petroleum ether. The combined organic phase was dried over MgSO₄, filtered and the solvent removed. The residue was purified by chromatography on silica gel with petroleum ether–ethyl acetate (*v/v* = 10:1) to give 4-bromo-2,6-diethylaniline (0.94 g, 83% yield). ¹H NMR (400 MHz, CDCl₃): δ 7.06 (s, 2H, aniline ring), 3.59 (br, s, 2H, –NH₂), 2.48 (q, *J* = 7.1 Hz, 4H, –CH₂CH₃), 1.24 (t, *J* = 7.1 Hz, 6H, –CH₂CH₃). ¹³C NMR (100 MHz, CDCl₃): δ 141.77 (aniline carbon connected with NH₂), 129.79 (aniline carbon near Br), 128.61 (aniline carbon connected with ethyl), 110.43 (aniline carbon connected with Br), 24.25 (–CH₂CH₃), 12.91 (–CH₂CH₃). 7.06 (s, 2H, aniline ring), 3.59 (br, s, 2H, –NH₂), 2.48 (q, *J* = 7.1 Hz, 4H, –CH₂CH₃), 1.24 (t, *J* = 7.1 Hz, 6H, –CH₂CH₃). Anal. Calcd for C₁₀H₁₄BrN: C, 52.65; H, 6.19; N, 6.14. Found: C, 52.37; H, 6.37; N, 6.29. FT-IR (KBr) 3361 cm⁻¹, 3438 cm⁻¹ (–NH₂).

Synthesis of 2,6-diethyl-4-naphthylaniline **1a**

Pd(OAc)₂ (0.01 g, 0.04 mmol), 4-bromo-2,6-diethylaniline (0.46 g, 2.00 mmol), K₂CO₃ (0.55 g, 4.00 mmol) and 1-naphthyl boric acid (0.38 g, 2.20 mmol) were placed in a 50 ml flask and stirred at 25°C for 24 h, in the presence of 10 ml PEG-400. The mixture was extracted three times with 15 ml diethyl ether. The combined organic phase was dried over MgSO₄, filtered and the solvent was removed. The residue was purified by chromatography on silica gel with petroleum ether–ethyl acetate (*v/v*, 30:1) to give

2,6-diethyl-4-naphthylaniline (0.41 g, 74% yield). ¹H NMR (400 MHz, CDCl₃): δ 8.08 (d, *J* = 7.8 Hz, 1H, naphthyl), 7.91 (d, *J* = 8.0 Hz, 1H, naphthyl), 7.83 (d, *J* = 6.8 Hz, 1H, naphthyl), 7.43–7.55 (m, 4H, naphthyl), 7.18 (s, 2H, aniline), 3.72 (br, s, 2H, –NH₂), 2.64 (q, *J* = 7.1 Hz, 4H, –CH₂CH₃), 1.34 (t, *J* = 7.1 Hz, 6H, –CH₂CH₃). ¹³C NMR (100 MHz, CDCl₃): δ 140.42 (aniline carbon connected with NH₂), 133.51 (naphthyl carbon connected with aniline), 130.19 (naphthyl carbon), 128.32 (naphthyl carbon), 128.14 (naphthyl carbon), 128.05 (naphthyl carbon), 127.75 (naphthyl carbon), 127.31 (aniline carbon), 126.99 (naphthyl carbon), 126.41 (naphthyl carbon), 126.36 (naphthyl carbon), 126.00 (naphthyl carbon), 125.74 (aniline carbon connected with naphthyl), 125.21 (aniline carbon connected with ethyl), 23.92 (–CH₂CH₃), 12.66 (–CH₂CH₃). Anal. Calcd for C₂₀H₂₁BrN: C, 87.23; H, 7.69; N, 5.09. Found: C, 87.11; H, 7.81; N, 5.27. FT-IR (KBr) 3369 cm⁻¹, 3441 cm⁻¹ (–NH₂).

Synthesis of 4-fluoro-2-methyl-6-sec-phenethylaniline **1b**

CF₃SO₃H (0.06 g, 0.40 mmol), 4-fluoro-2-methylaniline (0.25 g, 2.00 mmol), styrene (0.42 g, 4.00 mmol) and xylene (2 ml) were placed in a 10 ml Schlenk flask and stirred at 160°C for 8 h. Volatile materials were removed and the residue was purified by chromatography on silica gel with petroleum ether–ethyl acetate (*v/v*, 10:1) to give 4-fluoro-2-methyl-6-sec-phenethylaniline as light-yellow oil (0.32 g, 70% yield). ¹H NMR (400 MHz, CDCl₃): δ 7.12–7.23 (m, 5H, C₆H₅CHCH₃), 6.83 (s, 2H, aniline ring), 6.64 (s, 2H, aniline ring), 3.96 (q, *J* = 7.1 Hz, 1H, C₆H₅CHCH₃), 3.13 (br, s, 2H, –NH₂), 2.00 (s, 3H, –CH₃ of aniline), 1.50 (d, *J* = 7.1 Hz, 3H, C₆H₅CHCH₃). ¹³C NMR (100 MHz, CDCl₃): δ 157.02 (aniline carbon connected with fluorine), 154.68 (phenethyl ring carbon connected with ethyl), 144.88 (aniline carbon connected with NH₂), 138.10 (aniline carbon connected with methyl), 130.51 (phenyl carbon), 128.62 (phenyl carbon), 127.35 (phenyl carbon), 126.34 (aniline carbon connected with phenethyl), 114.71 (aniline carbon near methyl), 111.30 (aniline carbon near F), 40.26 (C₆H₅CHCH₃), 21.90 (C₆H₅CHCH₃), 17.53 (–CH₃ of aniline). Anal. Calcd for C₁₅H₁₆FN: C, 78.57; H, 7.03; N, 6.11. Found: C, 78.62; H, 6.89; N, 5.97. FT-IR (KBr) 3381 cm⁻¹, 3443 cm⁻¹ (–NH₂).

Synthesis of 4-fluoro-6-sec-phenethylaniline **1c** or **1d**

Using the same procedure as for the synthesis of **1b**, **1c/1d** was obtained as a light-yellow oil (0.52 g, 60% yield). ¹H NMR (400 MHz, CDCl₃): δ 7.15–7.27 (m, 5H, C₆H₅CHCH₃), 7.01 (s, 1H, aniline ring), 6.77 (d, *J* = 8.4 Hz, 1H, aniline ring), 6.51 (d, *J* = 8.6 Hz, 1H, aniline ring), 4.02 (q, *J* = 7.1 Hz, 1H, C₆H₅CHCH₃), 3.24 (br, s, 2H, –NH₂), 1.56 (d, *J* = 7.1 Hz, 3H, C₆H₅CHCH₃). ¹³C NMR (100 MHz, CDCl₃): δ 157.74 (aniline carbon connected with F), 144.78 (phenethyl ring carbon connected with ethyl), 140.15 (aniline carbon connected with NH₂), 128.72 (phenyl carbon), 127.28 (phenyl carbon), 126.46 (phenyl carbon), 116.73 (aniline carbon connected with phenethyl), 113.73 (aniline carbon), 113.40 (aniline carbon), 113.18 (aniline carbon), 40.07 (C₆H₅CHCH₃), 21.65 (C₆H₅CHCH₃). Anal. Calcd for C₁₄H₁₄FN: C, 78.11; H, 6.56; N, 6.51. Found: C, 77.94; H, 6.75; N, 6.82. FT-IR (KBr) 3374 cm⁻¹, 3439 cm⁻¹ (–NH₂).

Synthesis of bis[*N,N'*-(2,6-diethyl-4-naphthylphenyl)imino]-1,2-dimethylethane **2a**

Formic acid (0.5 ml) was added to a stirred solution of 2,3-butanedione (0.09 g, 1.00 mmol) and 2,6-diethyl-4-naphthylaniline (0.61 g, 2.2 mmol) in ethanol (20 ml). The mixture was refluxed for 48 h, then cooled and the precipitate was separated by filtration.

The solid was recrystallized from EtOH–CHCl₂ (v/v, 15:1), washed and dried under vacuum. Yield 0.33 g (55%). ¹H NMR (400 MHz, CDCl₃): δ 8.03 (d, *J* = 8.0 Hz, 2H, γ-naphthyl), 7.94 (d, *J* = 8.2 Hz, 2H, α-naphthyl), 7.86 (d, *J* = 8.3 Hz, 2H, β-naphthyl), 7.47–7.56 (m, 8H, naphthyl), 7.28 (s, 4H, aniline ring), 2.40–2.58 (m, 4H, –CH₂CH₃ of aniline), 2.23 (s, 6H, –N=C(CH₃)C(CH₃)=N–), 1.22–1.27 (m, 12H, –CH₂CH₃ of aniline). ¹³C NMR (100 MHz, CDCl₃): δ 168.09 (C=N), 146.37 (aniline carbon connected with N), 140.50 (naphthyl carbon connected with aniline), 135.72 (aniline carbon connected with naphthyl), 133.70 (aniline carbon connected with ethyl), 131.70 (naphthyl carbon), 130.22 (naphthyl carbon), 128.29 (naphthyl carbon), 127.89 (naphthyl carbon), 127.68 (aniline carbon), 126.88 (naphthyl carbon), 126.27 (naphthyl carbon), 125.89 (naphthyl carbon), 125.68 (naphthyl carbon), 125.44 (naphthyl carbon), 24.62 (–CH₂CH₃ of aniline), 16.30 (–CH₂CH₃ of aniline), 13.54 (–N=C(CH₃)C(CH₃)=N–). Anal. Calcd for C₄₄H₄₄N₂: C, 87.96; H, 7.38; N, 4.66. Found: C, 87.79; H, 7.51; N, 4.82. FT-IR (KBr) 1645 cm^{–1} (C=N).

Synthesis of bis[N,N'-(4-fluoro-2-methyl-6-sec-phenethylphenyl)imino]-1,2-dimethylethane **2b**

Using the same procedure as for the synthesis of **2a**, **2b** was obtained as a yellow powder (0.26 g, 51% yield). ¹H NMR (400 MHz, CDCl₃): δ 7.14–7.17 (m, 10H, C₆H₅CHCH₃), 6.96 (s, 2H, aniline ring), 6.84 (s, 2H, aniline ring), 3.88 (q, *J* = 7.1 Hz, 2H, C₆H₅CHCH₃), 1.99 (s, 6H, –CH₃ of aniline), 1.51 (d, *J* = 7.1 Hz, 6H, C₆H₅CHCH₃), 1.18 (s, 6H, –N=C(CH₃)C(CH₃)=N–). ¹³C NMR (100 MHz, CDCl₃): δ 161.01 (C=N), 159.77 (aniline carbon connected with F), 143.71 (aniline carbon connected with N), 138.22

(phenylethyl ring carbon connected with ethyl), 137.31 (aniline carbon connected with phenylethyl), 125.78 (aniline carbon connected with methyl), 129.62 (phenyl carbon), 128.33 (phenyl carbon), 124.14 (phenyl carbon), 124.28 (aniline carbon), 113.63 (aniline carbon), 34.12 (C₆H₅CHCH₃), 22.79 (C₆H₅CHCH₃), 21.36 (–CH₃ of aniline), 15.78 (–N=C(CH₃)C(CH₃)=N–). Anal. Calcd for C₃₄H₃₄F₂N₂: C, 80.28; H, 6.74; N, 5.51. Found: C, 80.35; H, 6.58; N, 5.42. FT-IR (KBr) 1642 cm^{–1} (C=N). Single crystals of ligand **2b** suitable for X-ray analysis were obtained at –30°C by dissolving the ligand in CH₂Cl₂, followed by careful layering of the resulting solution with *n*-hexane.

Synthesis of bis[N,N'-(4-fluoro-6-sec-phenethylphenyl)imino]-1,2-dimethylethane **2c or **2d****

Using the same procedure as for the synthesis of **2a**, **2c/2d** was obtained as an orange powder (0.28 g, 58% yield). ¹H NMR (400 MHz, CDCl₃): δ 7.28 (s, 2H, aniline ring), 7.08–7.22 (m, 10H, C₆H₅CHCH₃), 7.04 (d, *J* = 8.0 Hz, 2H, aniline ring), 6.92 (d, *J* = 8.0 Hz, 2H, aniline ring), 4.08 (q, *J* = 6.9 Hz, 2H, C₆H₅CHCH₃), 1.51–1.63 (m, 12H, C₆H₅CHCH₃ and –N=C(CH₃)C(CH₃)=N–). ¹³C NMR (100 MHz, CDCl₃): δ 168.26 (C=N), 154.87 (aniline carbon connected with F), 145.94 (phenethyl ring carbon connected with ethyl), 145.26 (aniline carbon connected with N), 137.31 (aniline carbon connected with phenylethyl), 128.67 (phenyl carbon), 128.07 (phenyl carbon), 127.37 (phenyl carbon), 126.36 (aniline carbon), 125.84 (aniline carbon), 118.74 (aniline carbon), 39.04 (C₆H₅CHCH₃), 21.18 (C₆H₅CHCH₃), 15.78 (–N=C(CH₃)C(CH₃)=N–). Anal. Calcd for C₃₂H₃₀F₂N₂: C, 79.97; H, 6.29; N, 5.83. Found: C, 80.13; H, 6.15; N, 5.68. FT-IR (KBr) 1641 cm^{–1} (C=N).

Table 1. Crystal data and refinement details for **2b**, **3a**, **3c** and **3d**

Complex	2b	3a	3c	3d
Empirical Formula	C ₃₄ H ₃₄ F ₂ N ₂	C ₄₄ H ₄₄ Br ₂ N ₂ Ni ₂ (CH ₂ Cl ₂)	C ₃₂ H ₃₀ Br ₂ F ₂ N ₂ Ni	C ₃₂ H ₃₀ Cl ₂ F ₂ N ₂ Pd
Formula mass	508.63	989.19	699.11	657.88
Temperature (K)	296	150	293	296
Wavelength (Å)	0.71073	1.54180	0.7107	0.71070
Crystal size (mm ³)	0.19 × 0.21 × 0.23	0.16 × 0.17 × 0.29	0.28 × 0.22 × 0.21	0.08 × 0.25 × 0.38
Crystal system	Monoclinic	Monoclinic	Orthorhombic	Orthorhombic
Space group	<i>P</i> 2 ₁ / <i>n</i>	<i>I</i> 2/ <i>c</i>	<i>P</i> 2 ₁ <i>n</i> a	<i>P</i> <i>b</i> <i>c</i> <i>n</i>
<i>a</i> (Å)	11.166(15)	16.6851(8)	8.3327(15)	23.9837(4)
<i>b</i> (Å)	9.586(12)	13.5166(6)	25.221 (6)	17.2483(3)
<i>c</i> (Å)	13.469(18)	19.1448(11)	14.532(3)	28.7724(5)
(°)	94.160(13)	92.797(5)	90	90
<i>V</i> (Å ³)	1438(3)	4312.5(4)	3054.0(12)	11902.5(3)
<i>Z</i>	2	4	2	16
Density (calcd) (mg cm ^{–3})	1.175	1.524	0.760	1.469
Absorption coefficient (mm ^{–1})	0.077	5.365	1.64	0.839
<i>F</i> (000)	540	2 016	704	5 344
Theta range for data collec. (°)	2.3–25.5	4.0–70.1	3.5–25.5	3.0–26.0
Reflections collected	9890	12 157	8614	54 798
Independent reflections	2671	4 097	4428	11 703
Reflections with <i>I</i> > 2 (<i>I</i>)	1670	3 684		8 523
<i>R</i> _{int}	0.037	0.038	0.122	0.048
Final <i>R</i> indices [<i>I</i> > 2 (<i>I</i>)]	<i>R</i> ₁ = 0.044 <i>wR</i> ₂ = 0.099	<i>R</i> ₁ = 0.058 <i>wR</i> ₂ = 0.164	<i>R</i> ₁ = 0.1481 <i>wR</i> ₂ = 0.3486	<i>R</i> ₁ = 0.043 <i>wR</i> ₂ = 0.074
<i>R</i> indices (all data)	<i>R</i> ₁ = 0.089 <i>wR</i> ₂ = 0.139	<i>R</i> ₁ = 0.064 <i>wR</i> ₂ = 0.167	<i>R</i> ₁ = 0.1633 <i>wR</i> ₂ = 0.3665	<i>R</i> ₁ = 0.068 <i>wR</i> ₂ = 0.084
Goodness of fit on <i>F</i> ²	1.09	1.19	1.17	1.13
Largest diff. peak and hole (e Å ^{–3})	0.18 and –0.19	1.19 and –0.18	2.51 and –1.28	0.61 and –0.45

Synthesis of bis[*N,N'*-(2,6-dimethylphenyl)imino]-1,2-dimethylethane **2e**

Bis[*N,N'*-(2,6-dimethylphenyl)imino]-1,2-dimethylethane **2e** was synthesized according to the literature.^[27]

Synthesis of {bis[*N,N'*-(2,6-diethyl-4-naphthylphenyl)imino]-1,2-dimethylethane}dibromonickel **3a**

NiBr₂(DME) (0.31 g, 1.00 mmol), ligand **2a** (0.60 g, 1.00 mmol) and dichloromethane (40 ml) were mixed in a Schlenk flask and stirred at room temperature for 24 h. The resulting suspension was filtered. The solvent was removed under vacuum and the residue was washed with diethyl ether (3 × 15 ml), and then dried under vacuum at room temperature to give complex **3a** as light-brown micro-crystals (0.79 g, 81% yield). Anal. Calcd for C₄₄H₄₄Br₂N₂Ni·2(CH₂Cl₂): C, 55.48; H, 4.66; N, 2.88. Found: C, 55.59; H, 4.81; N, 2.93. FT-IR (KBr) 1648 cm⁻¹ (C=N). Single crystals of complex **3a** suitable for X-ray analysis were obtained at -30°C by dissolving the complex in CH₂Cl₂, followed by careful layering of the resulting solution with *n*-hexane.

Synthesis of {bis[*N,N'*-(4-fluoro-2-methyl-6-phenethylphenyl)imino]-1,2-dimethylethane}dibromonickel **3b**

Using the same procedure as for the synthesis of **3a**, **3b** was obtained as brown micro-crystals (0.62 g, 85% yield). Anal. Calcd

for C₃₄H₃₄Br₂F₂N₂Ni: C, 56.16; H, 4.71; N, 3.85. Found: C, 56.22; H, 4.84; N, 3.72. FT-IR (KBr) 1646 cm⁻¹ (C=N).

Synthesis of {bis[*N,N'*-(4-fluoro-6-phenethylphenyl)imino]-1,2-dimethylethane}dibromonickel **3c**

Using the same procedure as for the synthesis of **3a**, **3c** was obtained as dark-brown micro-crystals (0.54 g, 77% yield). Anal. Calcd for C₃₂H₃₀Br₂F₂N₂Ni: C, 54.98; H, 4.33; N, 4.01. Found: C, 55.07; H, 4.21; N, 3.88. FT-IR (KBr) 1656 cm⁻¹ (C=N). Single crystals of complex **3c** suitable for X-ray analysis were obtained at -30°C by dissolving the complex in CH₂Cl₂, followed by careful layering of the resulting solution with *n*-hexane.

Synthesis of {bis[*N,N'*-(4-fluoro-6-phenethylphenyl)imino]-1,2-dimethylethane}dichloropalladium **3d**

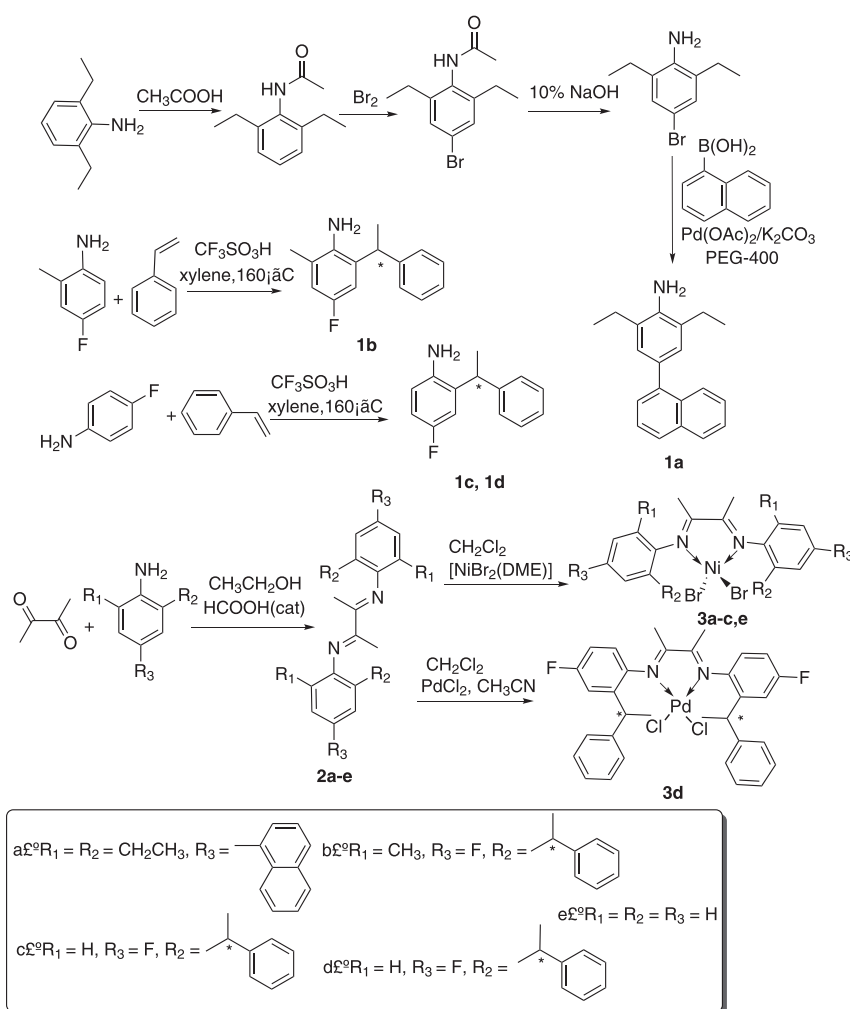
PdCl₂ (0.20 g, 1.13 mmol), ligand **2d** (0.48 g, 1.00 mmol) and acetonitrile (40 ml) were mixed in a Schlenk flask and refluxed under stirring for 30 min, then cooled down to room temperature. The resulting suspension was filtered. The solvent was removed under vacuum and the residue was washed with diethyl ether (3 × 15 ml), and then dried under vacuum at room temperature to give complex **3d** as light-yellow micro-crystals 0.58 g (88% yield). Anal. Calcd for C₃₂H₃₀Cl₂F₂N₂Pd: C, 58.42; H, 4.60; N, 4.26. Found: C, 58.53; H, 4.44; N, 4.12. FT-IR (KBr) 1644 cm⁻¹ (C=N). Single crystals of complex **3d** suitable for X-ray analysis were obtained at 15 °C by dissolving the complex in CH₂Cl₂, followed by careful layering of the resulting solution with *n*-hexane.

Synthesis of {bis[*N,N'*-(2,6-dimethylphenyl)imino]-1,2-dimethylethane}dibromonickel **3e**

{Bis[*N,N'*-(2,6-dimethylphenyl)imino]-1,2-dimethylethane}dibromonickel **3e** was synthesized according to the literature.^[27]

X-Ray Structure Determinations

For ligand **2b**, the data collection was performed at 296 K on a Bruker SMART APEX diffractometer with a CCD area detector, using graphite monochromated Mo-K_α radiation (λ = 0.71073 Å). The raw frame data were processed using SAINT^[28] and SADABS.^[28] SHELXTL^[29] was used for structure solving and refinement. For complex **3a**, data were collected on an Agilent Technologies SuperNova Eos Dual diffractometer using graphite monochromated Cu-K_α radiation (λ = 1.5418 Å); for complexes **3c** and **3d**, data were collected on an Agilent Technologies SuperNova Eos Dual diffractometer using graphite monochromated Mo-K_α radiation (λ = 0.71073 Å); CrysAlis PRO^[30] was used for cell refinement and data reduction at 150–296 K. The structures were solved by using SUPERFLIP^[31] and SHELXTL^[29] was used for the refinement. For complex **3a**, the residual electron density peaks greater than 1 e Å⁻³ were near bromide atoms. Crystal data and refinement parameters are listed in Table 1.



Scheme 1. Synthesis of ligands **2a–e** (*chiral carbon) and their corresponding α -diimine nickel(II) or palladium(II) complexes **3a–e**.

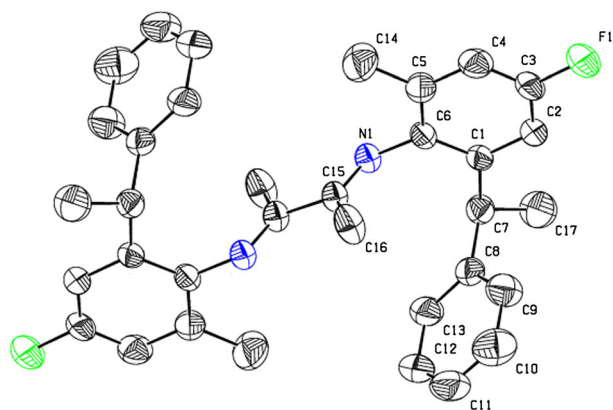


Figure 1. Molecular structure of ligand *rac*-(*RS*)-2b. Hydrogen atoms have been omitted for clarity. Selected bond lengths (Å) and angles (°): C15–C15a, 1.499 (4); C15–C16, 1.494(3); N1–C6, 1.419(3); N1–C15, 1.272 (3); C3–F1, 1.365(3); N1–C6–C1, 119.09 (18); N1–C6–C5, 119.32 (19); C6–N1–C15, 120.70(19). Symmetry code: (a) $-x+1, -y, -z$.

Procedure for the Polymerization of Ethylene

The polymerization of ethylene was carried out in a flame-dried 250 ml crown-capped pressure bottle sealed with neoprene septa. After drying the polymerization bottle under N_2 atmosphere, 50 ml dry toluene was added to the polymerization bottle. The resulting solvent was then saturated with a prescribed ethylene pressure. The co-catalyst (DEAC) was then added in Al/Ni or Al/Pd molar ratios in the range of 200–1000 to the polymerization bottle via a syringe. At this time, the solutions were thermostated to the desired temperature and allowed to equilibrate for 15 min. Subsequently, an *o*-dichlorobenzene solution of Ni or Pd catalyst was added to the polymerization reactor. The polymerization, conducted under a dynamic pressure of ethylene (0.2 bar), was terminated by quenching the reaction mixtures with 100 ml of a 2% HCl–MeOH solution. The precipitated polymer was filtered, washed with methanol and dried under vacuum at 60°C to a constant weight.

Procedure for the Polymerization of Styrene

The homopolymerization of styrene was carried out in a flame-dried 250 ml Schlenk flask under dry nitrogen in toluene at

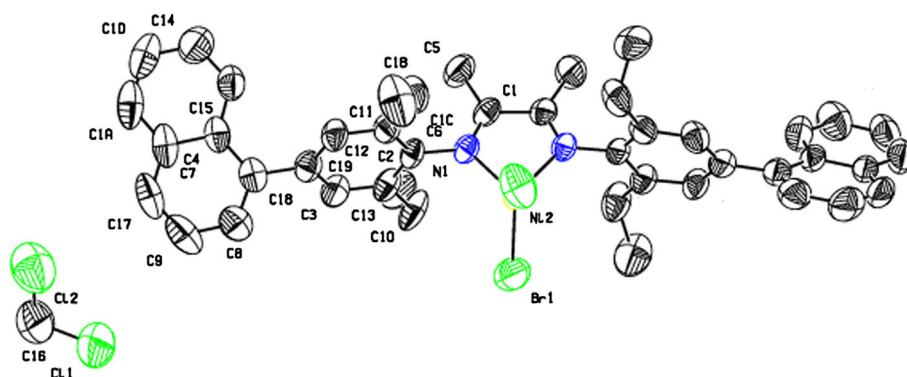


Figure 2. Molecular structure of complex **3a**. Hydrogen atoms have been omitted for clarity. Selected bond lengths (Å) and angles (°): Ni2–N1, 2.005(4); Ni2–Br1, 2.3316(8); N1–C6, 1.447(6); N1–C1, 1.281(6); N1–Ni2–N1a, 80.5(2); N1–Ni2–Br1, 108.86(11); N1a–Ni2–Br1, 114.16(11); N1–Ni2–Br1a, 114.16(11); N1a–Ni2–Br1a, 108.86(11); Br1–Ni2–Br1a, 122.64(6). Selected torsion angles (°): C2–C6–N1–Ni2, $-87.1(5)$; C12–C6–N1–Ni2, $89.6(5)$. Symmetry code: (a) $-x, y, -z+1/2$.

30–90°C. Dry toluene (25 ml) and dry styrene (5 ml) were added to the polymerization reactor; the co-catalyst (DEAC) was then added in Al/Ni or Al/Pd molar ratios in the range of 100–800 to the polymerization bottle via a syringe. Subsequently, an *o*-dichlorobenzene solution of Ni or Pd catalyst was added to the polymerization reactor. After a specific reaction time, the polymerization mixture was terminated by quenching the reaction mixtures with 100 ml of a 2% HCl–MeOH solution. The precipitated polymer was filtered, washed with methanol and dried under vacuum at 50°C to a constant weight.

Results and Discussion

Synthesis and Characterization of Ligands **2a–e** and complexes **3a–e**

The general synthetic route of the nickel(II) complexes **3a–e** are shown in Scheme 1. After protection of the amino group by acetic acid, 2,6-diethylaniline was brominated to form 4-bromo-2,6-diethylaniline **1a**. The Suzuki coupling reaction of 4-bromo-2,6-diethylaniline and 1-naphthyl boric acid catalyzed by Pd(OAc)₂ in PEG-400 led to the desired amine 2,6-diethyl-4-naphthylaniline **1a** in 74% yield. Reaction of 4-fluoro-2-methylamine and 4-fluoroamine with styrene at elevated temperature (160°C) in the presence of CF₃SO₃H catalyst resulted in the corresponding *o*-sec-phenethyl anilines *rac*-**1b** (70% yield) and *rac*-**1c/1d** (60% yield).

The α -diimine ligands (**2a–e**) were prepared by the condensation of equivalents of the appropriate aniline with 1 equiv. of 2,3-butanedione, usually in the presence of a formic acid catalyst. The ligands (**2a–e**) were characterized by ¹H NMR, ¹³C NMR and elemental analysis.

The reaction of equimolar amounts of NiBr₂ (DME) and the α -diimine ligands (**2a–c, e**) in CH₂Cl₂ led to the displacement of 1,2-dimethoxyethane and afforded the catalyst precursors (**3a–c, e**) as moderately air-stable microcrystalline solids in high yields. Complex *rac*-**3d** was prepared by refluxing PdCl₂ and ligand *rac*-**2d** in acetonitrile. These α -diimine Ni(II) complexes are paramagnetic, precluding measurement of their ¹H NMR spectra.

X-Ray Crystallographic Studies

The molecular structure of ligand *rac*-(*RS*)-**2b** (Fig. 1) was determined and selected bond distances and angles are given in the figure caption. The compound exhibits a *trans* conformation about the central C–C bond. Bond lengths and angles are within the expected range for α -diimines. For example, the bond distances for the C15=N1 double bond and the central C15–C15 single bond are 1.272(3) Å and 1.499(4) Å, respectively, which are very close to the values for other structurally characterized free α -diimines.^[32] Both C15 and C6 possess essentially rather planar geometry (sp^2 character), as shown by the C15–N1–C6 angles (120.70(19)°), which are very close to 120°.

The molecular structures of complexes **3a** (containing two dichloromethane molecules of crystallization) and *rac*-(*RR/SS*)-**3c** were also determined

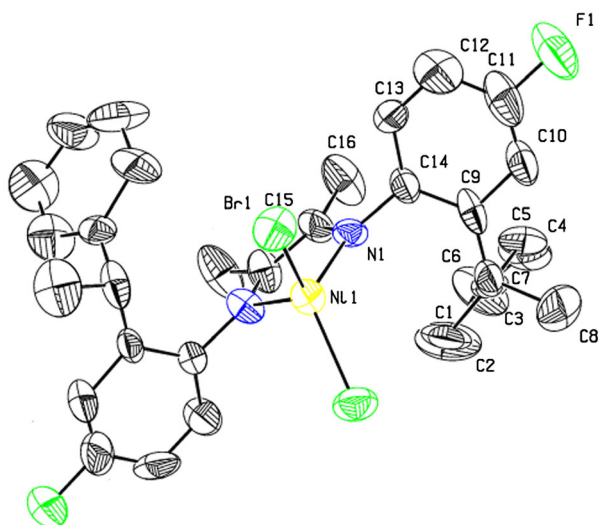


Figure 3. Molecular structure of complex *rac*-(*RR/SS*)-**3c**. Hydrogen atoms have been omitted for clarity. Selected bond lengths (Å) and angles (°): Ni1–N1, 1.982(12); Ni1–N1a, 1.982(12); Ni1–Br1, 2.327(2); N1–C14, 1.463(18); N1–C15, 1.31(2); C11–F1, 1.44(2); N1–Ni1–N1a, 79.3(7); N1–Ni1–Br1, 104.6(4); N1a–Ni1–Br1, 118.9(4); N1–Ni1–Br1a, 118.9(4); N1a–Ni1–Br1a, 104.6(4); Br1–Ni1–Br1a, 123.05(17). Selected torsion angles (°): C9–C14–N1–Ni1, 81.3(17); C13–C14–N1–Ni1, –101.4(18). Symmetry code: (a) *x*, –*y*, –*z*+1.

(Figs. 2 and 3), and selected bond distances and angles are given in the captions. The structures have pseudo-tetrahedral geometries and each shows crystallographic C_2 molecular symmetry. In the solid state, the most interesting feature of ligands **2a** and *rac*-(*RR/SS*)-**2c** are the conformation of the substituents attached to

N1. These groups are rotated about 180° from the position they must occupy to chelate metal Ni. The rotation has been confirmed by the crystal structure of their complexes **3a** and *rac*-(*RR/SS*)-**3c**. Both aryl rings bonded to the iminic nitrogens of the α -diimine lie nearly perpendicular to the plane formed by the nickel and coordinated nitrogen atoms (torsion angles for **3a**: C2–C6–N1–Ni2, $-87.1(5)^\circ$; C12–C6–N1–Ni2, $89.6(5)^\circ$; torsion angles for *rac*-(*RR/SS*)-**3c**: C9–C14–N1–Ni1, $81.3(17)^\circ$; C13–C14–N1–Ni1, $-101.4(18)^\circ$). The ethyl or chiral phenethyl groups in the 2,6-position of the aniline fragments in **3a** and *rac*-(*RR/SS*)-**3c** point toward each other above and below the plane, thus shielding the apical positions of the Ni(II) center. The axial sites for the metal center are almost blocked by the *ortho-sec*-phenethyl or ethyl substituents, which will play a critical role in maintaining high activity and obtaining high-molecular-weight polymers at elevated temperatures (see below). Their structures are similar to those reported in the literature for other similar [NiBr₂(α -diimine)] compounds characterized by X-ray diffraction, i.e. [bis(*N,N'*-4-bromo-2,6-dimethylphenyl)imino]acenaphthene]dibromonickel^[33] and [bis(*N,N'*-(2,4,6-trimethylphenyl)imino)acenaphthene]dibromonickel.^[34] In fact, the Ni–N bond distances in complexes **3a** and *rac*-(*RR/SS*)-**3c** are similar to those determined for these complexes, as are the Ni–Br bond distances.

Unlike the pseudo-tetrahedral geometry about the nickel center in *rac*-(*RR/SS*)-**3c**, the structure of palladium complex *rac*-(*RR/SS*)-**3d** features a pseudo-square planar geometry, with each of the two independent molecules (M1 and M2) showing non-crystallographic C_2 molecular symmetry. The existence of two types of isomeric forms *rac*-(*RR/SS*)-**3d**-M1 and *rac*-(*RR/SS*)-**3d**-M2 shows that *rac*-(*RR/SS*)-**3d** is a stereochemically non-rigid complex and can change slightly in solution (Fig. 4). The imino C=N bond length of *rac*-(*RR/SS*)-**3d** is slightly shorter than that of complex *rac*-(*RR/SS*)-**3c** due to the different metal atom. By contrast to *rac*-(*RR/SS*)-**3c**, both aryl rings bonded to the iminic nitrogens of the α -diimine lie splayed to the plane formed by the palladium and coordinated nitrogen atoms due to the pseudo-square planar geometry about the palladium center (torsion angles for *rac*-(*RR/SS*)-**3d**-M1: C2–C1–N1–Pd1, $108.2(3)^\circ$ and C6–C1–N1–Pd1, $-74.7(4)^\circ$; and for *rac*-(*RR/SS*)-**3d**-M2: C34–C33–N3–Pd2, $117.4(3)^\circ$; C38–C33–N3–Pd2, $-62.3(4)^\circ$). The axial sites in *rac*-(*RR/SS*)-**3d** are less blocked by the *ortho-sec*-phenethyl substituents compared with nickel complex *rac*-(*RR/SS*)-**3c**, which may be the reason that the palladium complex *rac*-(*RR/SS*)-**3d** showed low activity and low-molecular-weight polymer was obtained (see below).

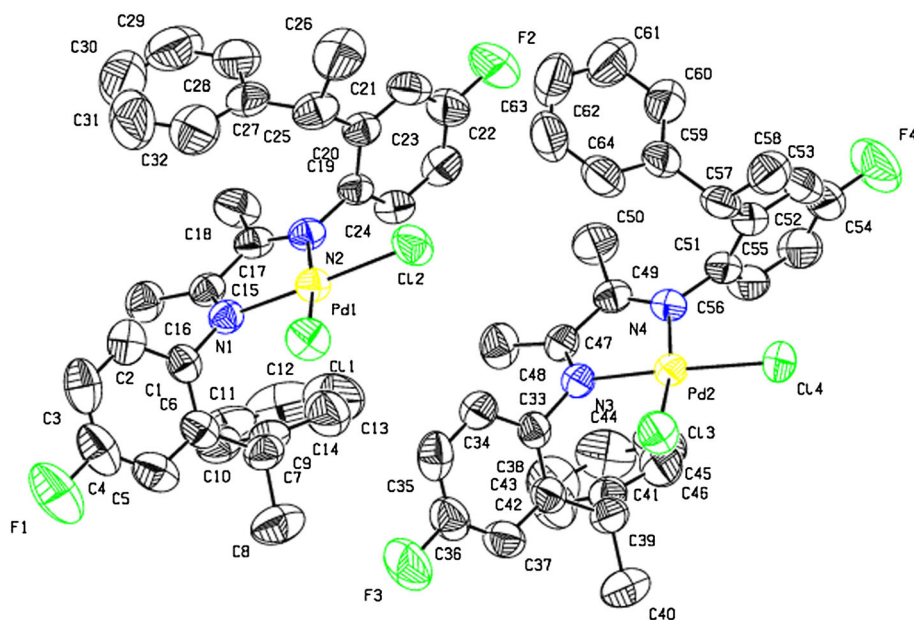


Figure 4. Molecular structure of complex *rac*-(*RR/SS*)-**3d**-M1 and *rac*-(*RR/SS*)-**3d**-M2. Hydrogen atoms have been omitted for clarity. Selected bond lengths (Å) and angles (°): Pd1–N1, 2.036(3); Pd1–N2, 2.023(3); Pd1–Cl1, 2.2845(10); Pd1–Cl2, 2.2750(11); N1–C1, 1.443(4); N1–C15, 1.292(4); Pd2–N3, 2.029(3); Pd2–N4, 2.029(3); Pd2–Cl3, 2.2773(10); Pd2–Cl4, 2.2799(10); N3–C33, 1.446(4); N3–C47, 1.296(4); N1–Pd1–N2, 79.39(12); N1–Pd1–Cl1, 96.05(9); N2–Pd1–Cl1, 173.52(9); N1–Pd1–Cl2, 173.05(9); N2–Pd1–Cl2, 93.99(9); Cl1–Pd1–Cl2, 90.72(4); N3–Pd2–N4, 79.29(12); N3–Pd2–Cl3, 95.00(9); N4–Pd2–Cl3, 169.76(9); N3–Pd2–Cl4, 171.28(9); N4–Pd2–Cl4, 95.92(9); Cl3–Pd2–Cl4, 90.78(4). Selected torsion angles (°): C2–C1–N1–Pd1, $108.2(3)^\circ$; C6–C1–N1–Pd1, $-74.7(4)^\circ$; C34–C33–N3–Pd2, $117.4(3)^\circ$; C38–C33–N3–Pd2, $-62.3(4)^\circ$.

Polymerization of Ethylene with Nickel Complexes **3a–e**

The five α -diimine nickel(II) complexes **3a–e**, activated by DEAC, were tested as catalyst precursors for the polymerization of ethylene, under the same reaction conditions. The results of the polymerization experiments are shown

Table 2. Polymerization of ethylene using complexes **3a**–**e**/DEAC catalytic systems^a

Run	Complex	[Al]/[M]	T (°C)	t (min)	Yield (g)	Activity ^b	TOF ^c	M _n ^d	M _w /M _n ^d	Branches ^e /1000 C
1	3a	200	10	10	1.826	3.74	1.34	7.28	1.71	—
2	3a	400	10	10	1.810	3.71	1.32	9.87	1.73	—
3	3a	600	10	10	2.223	4.56	1.63	10.12	2.03	—
4	3a	800	10	10	2.112	4.33	1.55	8.97	1.86	—
5	3a	1000	10	10	1.983	4.06	1.45	8.24	1.78	—
6	3a	600	0	10	1.145	2.35	0.84	11.14	1.74	—
7	3a	600	20	10	1.386	2.84	1.01	9.87	1.82	75.1
8	3a	600	40	10	0.734	1.50	0.54	6.15	1.95	97.4
9	3a	600	60	10	0.534	1.09	0.39	4.27	1.73	122.1
10	3b	600	0	10	2.539	5.20	1.86	13.35	1.98	—
11	3b	600	20	10	2.347	4.81	1.72	9.27	1.82	87.9
12	3b	600	40	10	1.752	3.59	1.28	8.26	2.07	106.5
13	3b	600	60	10	1.103	2.26	0.81	5.08	1.75	136.1
14	3c	600	0	10	0.700	1.44	0.51	8.73	1.94	—
15	3c	600	20	10	0.595	1.22	0.44	7.85	1.88	72.3
16	3c	600	40	10	0.471	0.97	0.34	5.65	1.87	90.8
17	3c	600	60	10	0.286	0.59	0.21	3.22	1.74	118.8
18	3d	200	10	60	0.153	0.05	0.02	1.17	1.91	—
19	3d	400	10	60	0.178	0.06	0.02	1.83	1.75	—
20	3d	600	10	60	0.324	0.11	0.04	2.27	2.11	—
21	3d	800	10	60	0.266	0.09	0.03	1.39	1.84	—
22	3d	1000	10	60	0.174	0.06	0.02	1.24	1.78	—
23	3d	600	0	60	0.202	0.07	0.02	2.11	1.96	—
24	3d	600	20	60	0.184	0.06	0.02	1.92	1.89	58.4
25	3d	600	40	60	0.141	0.05	0.02	1.21	1.95	64.9
26	3d	600	60	60	0.091	0.03	0.01	1.02	1.67	77.2
27	3e	600	0	10	0.648	1.33	0.47	9.83	2.19	—
28	3e	600	20	10	0.572	1.17	0.42	7.35	1.83	64.7
29	3e	600	40	10	0.415	0.85	0.30	5.78	1.87	71.2
30	3e	600	60	10	0.278	0.57	0.20	2.96	1.68	90.2

^aPolymerization conditions and definitions: $n(\mathbf{3a}) = n(\mathbf{3b}) = n(\mathbf{3c}) = n(\mathbf{3d}) = (\mathbf{3e}) = 2.44 \mu\text{mol}$; ethylene relative pressure = 0.2 bar, ethylene absolute pressure = 1.2 bar; t = polymerization time; solvent = toluene (50 ml); T = polymerization temperature.

^bActivity in $10^6 \text{ g PE (mol Ni h bar)}^{-1}$.

^cTurnover frequency in $10^5 \text{ mol ethylene (mol Ni h bar)}^{-1}$.

^d M_n in 10^4 g mol^{-1} , determined by GPC.

^eEstimated by $^1\text{H NMR}^{[35]}$ $\text{Branches}/1000 \text{ C} = \frac{\frac{1}{2}[\text{CH}_2]}{[\text{CH}_2 + \text{CH}_3 + 1]} \times 1000$

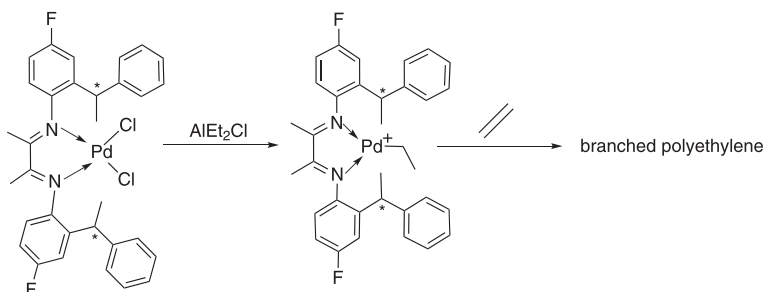
in Table 2. Noteworthy is the fact that blank experiments carried out with DEAC alone, under similar conditions, showed its inability to polymerize ethylene on its own. Four α -diimine Ni(II)/DEAC catalytic systems (**3a**/DEAC, *rac*-(*RS*)-**3b**/DEAC, *rac*-(*RR*/*SS*)-**3c**/DEAC and **3e**/DEAC) are highly active for ethylene polymerization; however, the α -diimine Pd(II)/DEAC catalytic system (*rac*-(*RR*/*SS*)-**3d**/DEAC)

shows significantly lower activity for ethylene polymerization compared with the α -diimine Ni(II)/DEAC catalytic systems.

At 10 °C, the activity of nickel complex **3a** increases slightly with the increase of [Al]/[Ni] ratio (runs 1–3), the maximum around [Al]/[Ni] ratio 600 (run 3), and then the activity decreases slightly with the increase of [Al]/[Ni] ratio (runs 3–6). For a ratio [Al]/[Ni] 600, the activity increases first up to 10 °C (runs 6 and 3) and then decreases slightly in the range 10–60 °C (runs 3, 7–9).

At 10 °C, the activity of nickel complex *rac*-(*RR*/*SS*)-**3d** increases slightly with the increase of [Al]/[Pd] ratio (runs 18–20), the maximum around [Al]/[Pd] ratio 600 (run 20), and then the activity decreases slightly with the increase of [Al]/[Pd] ratio (runs 20–22). For a ratio [Al]/[Pd] 600, the activity increases first up to 10 °C (runs 23 and 20) and then decreases slightly in the range 10–60 °C (runs 20, 22–26).

Performance of the nickel pre-catalysts are significantly affected by the *ortho* and *para* substituents on the aryl rings (Table 2). Complex *rac*-(*RS*)-**3b**, bearing



Scheme 2. Rationale for formation of the active species in ethylene polymerization catalyzed by palladium complex *rac*-(*RR*/*SS*)-**3d**.

one *ortho*-methyl, one bulky chiral *ortho-sec*-phenethyl and one strong electron-withdrawing *para*-fluorine group, displays the highest catalytic activity, 5.20×10^6 g PE (mol Ni h bar) $^{-1}$, and produces a chain of higher molecular weight (run 10, $M_n = 13.35 \times 10^4$ g mol $^{-1}$, 0°C, [Al]/[Ni] = 600) among the five complexes. Complex **3a**, bearing two *ortho*-ethyl groups and one bulky *para*-naphthyl group, also displays high catalytic activity (the highest activity: run 3, 4.56×10^6 g PE (mol Ni h bar) $^{-1}$, $M_n = 10.12 \times 10^4$ g mol $^{-1}$). This result shows that the rate of chain propagation could be better promoted by the bulky *ortho-sec*-phenethyl groups than the bulky *para*-naphthyl groups. A strong electron-withdrawing *para*-fluorine group of the ligand's aryl rings seems more favorable to promote chain growth rate.

Compared with *rac*-(*RS*)-**3b**, *rac*-(*RR/SS*)-**3c** (bearing one bulky chiral *ortho-sec*-phenethyl and a strong electron-withdrawing group *para*-fluorine) exhibits significantly lower catalytic activity (the highest activity: *rac*-(*RR/SS*)-**3c**, run 14, 1.44×10^6 g PE (mol Ni h bar) $^{-1}$) due to the absence *ortho*-methyl groups. This result indicates that the rate of chain propagation is greatly promoted by the bulky *ortho*-methyl groups of the ligand's aryl rings.

Compared with complexes **3a** and *rac*-(*RS*)-**3b**, complex **3e** (bearing two *ortho*-methyl groups) shows the lowest catalytic activity (highest activity: run 27, 1.33×10^6 g PE (mol Ni h bar) $^{-1}$) due to the absence of both *ortho*-position and *para*-position bulky groups.

Interestingly, the new chiral square planar α -diimine Pd(II) complex, *rac*-(*RR/SS*)-**3d**, also exhibits reasonably high activity toward ethylene polymerization [run 20, the highest activity: 0.11×10^6 g PE (mol Pd h bar) $^{-1}$; M_n 2.27×10^4 g mol $^{-1}$] under low ethylene pressure. These high activities may indicate that the active species operating in the case of pre-catalyst *rac*-(*RR/SS*)-**3d**, [PdCl $_2$ (Ar-DAB)], is the same as that revealed for the corresponding nickel(II) species [NiBr $_2$ (Ar-DAB)].¹⁷ The α -diimine Pd(II) complex used in the present work may be involved in a displacement of the ethyl group in DEAC to afford the active species for ethylene polymerization (Scheme 2). Of course, this displacement is difficult due to the poor leaving group Cl attached to palladium and the unfavorable molecular structure (see above); thus complex *rac*-(*RR/SS*)-**3d** showed significantly lower activity than those of complexes **3a**, *rac*-(*RS*)-**3b**, *rac*-(*RR/SS*)-**3c** and **3e**. As a result, the following activity trend can be summarized for our substituted pre-catalysts under low ethylene pressure (0.2 bar), in the range 0–60°C: **3b** > **3a** > **3c** ~ **3e** >> **3d**.

The type and amount of branches formed in the polymerization of ethylene promoted by typical α -diimine nickel/palladium pre-catalysts depend on reaction parameters such as the reaction temperature, ethylene pressure and ligand structure.¹⁷ Generally, low ethylene pressure and high polymerization temperature favor chain walking, and afford highly branched polyethylenes.¹⁷ However, the effect of ligand structure on polyethylene branching is much more complicated.

As shown in Table 2 and Fig. 5, the nickel catalyst system *rac*-(*RS*)-**3b**/DEAC generated polyethylene with the highest degrees of branching. The total branching degrees of polymer samples prepared with *rac*-(*RS*)-**3b**/DEAC (runs 11–13; branching degree: 87.9, 1026.5 and 136.1 branches/1000 C at 20, 40 and 60°C, respectively) are significantly higher than those observed for **3a**/DEAC (runs 7–9; branching degree: 75.1, 97.4 and 122.1 branches/1000 C at 20, 40 and 60°C, respectively), *rac*-(*RR/SS*)-**3c**/DEAC (runs 15–17; branching degree: 72.3, 90.8 and 118.8 branches/1000 C at 20, 40 and 60°C, respectively) and **3e**/DEAC systems (runs 28–30, branching degree: 64.7, 71.2 and 90.2 branches/1000 C at 20, 40 and 60°C, respectively). Also, the total branching degrees of polymer samples prepared with *rac*-(*RS*)-**3b**/DEAC are higher than those observed for similar pre-catalyst/DEAC systems such as {bis[*N,N'*-(4-*tert*-butyl-diphenyl)silyl-2,6-diisopropylphenyl]imino}acenaphthene}dibromonickel (45 branches/1000 C, at 20°C)¹⁷ or pre-catalyst/MAO systems such as {bis[*N,N'*-(2,6-diisopropylphenyl)imino]-1,2-dimethylethane}dibromonickel (30, 67, 80 and 90 branches/1000 C, at 25, 50, 65 and 80°C, respectively)¹⁷ and {bis[*N,N'*-(2,6-diisopropylphenyl)imino]acenaphthene}dibromonickel (65 branches/1000 C, at 25°C),¹⁷ although the reaction conditions are not exactly the same as in the present work. The total branching degree of the polymer sample obtained with **3e** bearing two electron-donating *ortho*-methyl groups is the lowest among our four nickel complexes. Our results (Table 2) are consistent in that the more electron-deficient catalyst affords a more branched polymer.¹⁶ A possible explanation is that a more electron-deficient ligand may better stabilize the transition state for monomer chain walking than for insertion, which should afford a more branched polymer.

Interestingly, compared with the nickel complexes, the palladium complex *rac*-(*RR/SS*)-**3c**/DEAC system produced polyethylene with much lower degrees of branching (runs 24–26, branching degree: 58.4, 64.9 and 77.2 branches/1000 C at 20, 40 and 60°C, respectively).

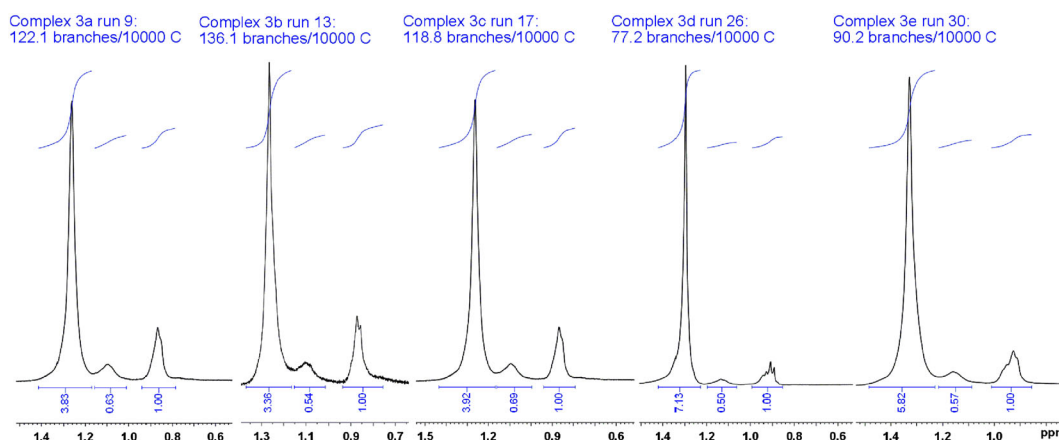


Figure 5. ^1H NMR (400 MHz, $\text{CDCl}_3/1,2,4$ -trichlorobenzene, $v/v = 1:3$) spectra of the polyethylenes catalyzed by **3a–e**/DEAC at 60°C (Table 2, runs 9, 13, 17, 26 and 30). I_{CH_3} : integrated intensity between 0.8 and 1.0 ppm; $I_{\text{CH}_2} + I_{\text{CH}}$: integrated intensity between 1.0 and 1.5 ppm.

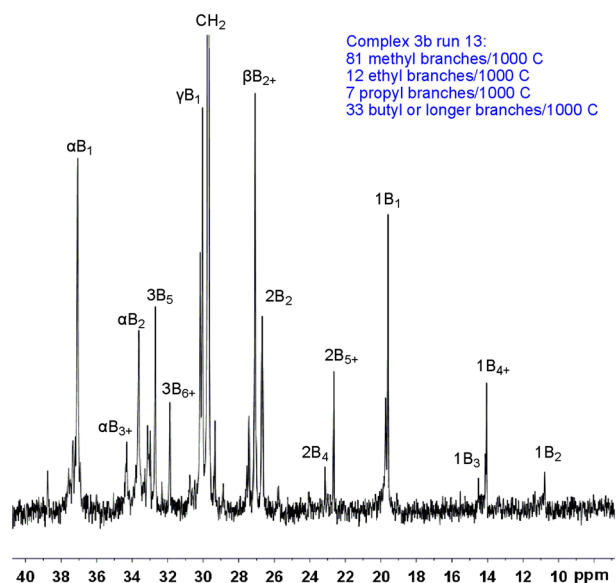


Figure 6. ^{13}C NMR (CDCl_3 /*o*-dichlorobenzene, $v/v = 1:3$) spectrum of polyethylene catalyzed by *rac*-(*RS*)-**3b**/DEAC at 60°C (Table 2, run 13). Note on labels $x\text{B}_y$: B_y is a branch of length y carbons; x is the carbon being discussed, and the methyl at the end of the branch is numbered 1. Thus the second carbon from the end of a butyl branch is 2B_4 . $x\text{B}_{y+}$ refers to branches of length y and longer. The methylene groups in the backbone are labeled with Greek letters which determine how far from a branch point methine each methylene is; α denotes the first methylene next to the methine. Thus γB_{1+} refers to methylenes γ from a branch of length 1 or longer.

The ^{13}C NMR spectrum of the polyethylene prepared with the catalyst *rac*-(*RS*)-**3b**/DEAC at 60°C is shown in Fig. 6. The number of branches was calculated according to the literature,^[36] and it was found that the polyethylene with 133 branches/1000 carbons (81 methyl, 12 ethyl, 7 propyl and 33 butyl or longer branches/1000 C) was obtained at 60°C (run 13 in Table 2). This result was consistent with that calculated from ^1H NMR.

Polymerization of styrene with nickel or palladium complexes **3a–d**

Polymerizations of styrene with complexes **3a–d** in combination with DEAC were carried out at 30–90°C, and the results are summarized in Table 3. At 30°C, activity of complexes **3a** increases slightly with the increase of $[\text{Al}]/[\text{Ni}]$ ratio (runs 1–4), the maximum around $[\text{Al}]/[\text{Ni}]$ ratio 600 (run 4), and then the activity decreases slightly with the increase of $[\text{Al}]/[\text{Ni}]$ ratio (runs 4 and 5). For a $[\text{Al}]/[\text{Ni}]$ ratio of 600, the activity of complex **3a–d** increases slightly with the increase of temperature (30–70°C), the maximum around 70°C, and then the activity decreases slightly with the increase of temperature (70–90°C). Molecular weight decreases significantly with the increase of polymerization temperature (30–90°C). Three α -diimine Ni(II)/DEAC catalytic systems (**3a**/DEAC, *rac*-(*RS*)-**3b**/DEAC and *rac*-(*RR/SS*)-**3c**/DEAC) are highly active for styrene polymerization; however, the α -diimine Pd(II)/DEAC catalytic system (*rac*-(*RR/SS*)-**3d**/DEAC) shows significantly lower activity for styrene polymerization compared with the α -diimine Ni(II)/DEAC catalytic systems. Complex *rac*-(*RS*)-**3b**

Table 3. Polymerization of styrene with nickel complexes **3a–d**/DEAC catalytic systems^a

Entry	Complex	$[\text{Al}]/[\text{M}]$	T (°C)	Yield (g)	Activity ^b	M_n^c	M_w/M_n^c	Triad fractions ^d (%)			Diad fractions ^e (%)	
								rr	mr	mm	r	m
1	3a	100	30	0.41	0.82	2.32	2.25					
2	3a	200	30	0.45	0.90	2.29	2.11					
3	3a	400	30	0.77	1.55	2.19	2.03					
4	3a	600	30	0.89	1.78	2.19	1.99					
5	3a	800	30	0.81	1.62	1.92	2.07					
6	3a	600	50	1.02	2.04	1.87	1.92					
7	3a	600	70	1.39	2.78	1.57	1.90	35.5	31.9	32.6	51.5	48.5
8	3a	600	90	1.24	2.48	1.03	2.02					
9	3b	600	30	0.73	1.46	2.51	2.11					
10	3b	600	50	1.09	2.18	2.03	2.15					
11	3b	600	70	1.41	2.82	1.64	2.08	44.2	31.7	24.0	60.1	39.9
12	3b	600	90	1.28	2.56	1.17	1.94					
13	3c	600	30	0.33	0.66	1.89	2.26	41.1	29.1	28.8	55.7	44.3
14	3c	600	50	0.74	1.48	1.43	2.17					
15	3c	600	70	0.98	1.96	1.25	2.08	40.2	29.6	30.2	55.0	45.0
16	3c	600	90	0.86	1.72	0.87	1.89					
17	3d	600	30	0.09	0.19	1.29	1.97					
18	3d	600	50	0.15	0.31	1.07	1.89					
19	3d	600	70	0.48	0.96	0.92	1.82	40.5	29.0	30.5	55.0	45.0
20	3d	600	90	0.46	0.92	0.75	1.85					

^aPolymerization conditions: $n(\mathbf{3a}) = n(\mathbf{3b}) = n(\mathbf{3d}) = 5 \mu\text{mol}$; 5 ml styrene; solvent: toluene (25 ml); T = polymerization temperature; polymerization time: 1 h.

^bActivity in 10^5 g polystyrene $(\text{mol Ni h})^{-1}$.

^c M_n in 10^4 g mol^{-1} , determined by GPC.

^dObserved in ^{13}C NMR spectra of quaternary carbon resonance, from low to high field in the spectra (δ 147–144 ppm).^[37–40]

^eCalculated from: $(m) = (mm) + 0.5 (mr)$.

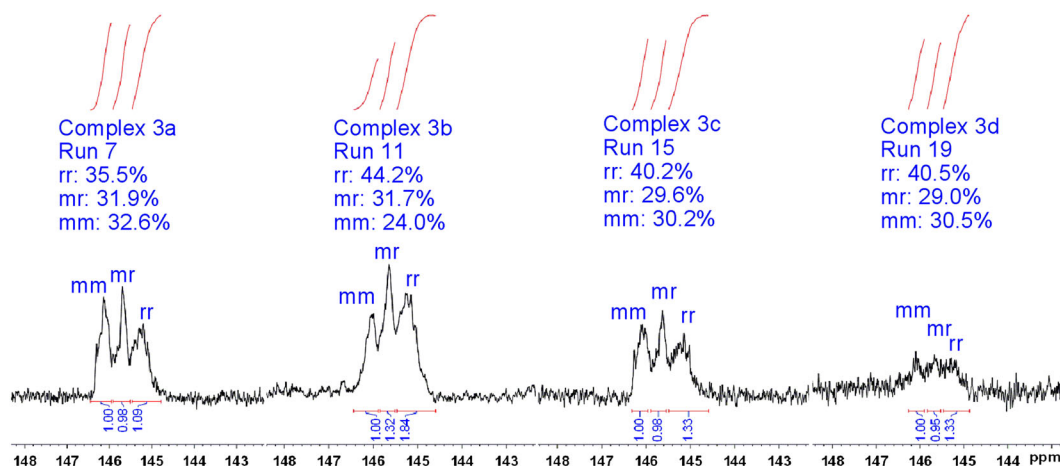


Figure 7. ^{13}C NMR (CDCl_3) spectra of the polystyrenes catalyzed by **3a–d**/DEAC at 70 °C.

displays the highest catalytic activity (2.82×10^5 g polystyrene $(\text{mol Ni h})^{-1}$) among our four complexes. Complex **3a** also displays high catalytic activity (highest activity: run 7, 2.78×10^5 g polystyrene $(\text{mol Ni h})^{-1}$). Compared with complex *rac*-(*RS*)-**3b**, complex *rac*-(*RR/SS*)-**3c** exhibits significantly lower catalytic activity (highest activity: nickel complex *rac*-(*RR/SS*)-**3c**/DEAC, run 15, 1.96×10^5 g polystyrene $(\text{mol Ni h})^{-1}$) due to the absence of *ortho*-methyl groups. This result indicates that the rate of chain propagation is greatly promoted by the bulky *ortho*-methyl groups of the ligand's aryl rings.

The *rac*-(*RR/SS*)-**3d** complex exhibits significantly low activity toward styrene polymerization (highest activity: run 19, 0.96×10^5 g polystyrene $(\text{mol Ni h})^{-1}$) due to its bad leaving group Cl attached to palladium and the unfavorable molecular structure. Also, at high temperature (70 and 90 °C), some of the zero-valent palladium precipitated due to decomposition of the catalyst.

The aromatic *ipso* carbon spectra of the polystyrenes obtained with catalysts **3a**, *rac*-(*RS*)-**3b**, *rac*-(*RR/SS*)-**3c** and *rac*-(*RR/SS*)-**3d**/DEAC were analyzed in term of triads. The three main signals, at 144.8–145.4, 145.5–145.9 and 146.0–146.4 ppm, are assigned to syndiotactic (*rr*), heterotactic (*mr*) and isotactic triads (*mm*), respectively.^[37–40] As in Table 3 and Fig. 7, chiral catalyst *rac*-(*RS*)-**3b** generated polystyrene with the highest degrees of stereoregularity. The stereoregularity degrees of the polymer sample prepared with *rac*-(*RS*)-**3b**/DEAC (stereo-triad distributions run 11: *rr*, 44.2%; *mr*, 31.7%; *mm*, 24.0%; stereo-diad distributions: *r*, 60.1%; *m*, 39.9% at 70 °C) are significantly higher than those observed for **3a**/DEAC (stereo-triad distributions run 7: *rr*, 35.5%; *mr*, 31.9%; *mm*, 32.6%; stereo-diad distributions: *r*, 51.5%; *m*, 48.5% at 70 °C), *rac*-(*RR/SS*)-**3c**/DEAC (stereo-triad distributions run 15: *rr*, 40.2%; *mr*, 29.6%; *mm*, 30.2%; stereo-diad distributions: *r*, 55.0%; *m*, 45.0% at 70 °C), and *rac*-(*RR/SS*)-**3d**/DEAC (stereo-triad distributions run 19: *rr*, 40.5%; *mr*, 29.0%; *mm*, 30.5%; stereo-diad distributions: *r*, 55.0%; *m*, 45.0% at 70 °C). The achiral catalyst **3a** gave nearly atactic polystyrene at 70 °C. Perhaps an aryl ligand bearing chiral bulky *sec*-phenethyl and strong withdrawing F groups in the *ortho* and *para*-aryl position may better control the stereoselective monomer insertion, which should afford a highly syndiotactic polystyrene. It is noteworthy that the impact of metal palladium and nickel on stereoregularity of polystyrene is very small (run 15 *rac*-(*RR/SS*)-**3c** and run 19 *rac*-(*RR/SS*)-**3d**).

A decrease in the reaction temperature has a minor influence on the sequence distribution (Table 3: runs 13 and 15, performed with *rac*-(*RR/SS*)-**3c**/DEAC at 30 and 70 °C, respectively) as a slight increase in the syndiotactic content is observed (at 30 °C run 13, stereo-triad distributions: *rr*, 41.1%; *mr*, 29.1%; *mm*, 28.8%; stereo-diad distributions: *r*, 55.7%; *m*, 44.3%).

Conclusions

A series of new α -diimine ligands **2a–e** and their Ni(II) or Pd(II) complexes **3a–e** have been prepared and characterized. Ligands **2a–e** were modified in an attempt to change the chiral environment, steric effects, electronic density of the metal center and metal atom (Ni or Pd), eventually to improve activity in the polymerization of ethylene/styrene and control the microstructure of polyethylene, in particular the stereoregularity structure of polystyrene. The results obtained show that the chiral nickel complex *rac*-(*RS*)-**3b** produces a highly active catalyst system for the polymerization of ethylene and highly branched polyethylene due to its bulky *ortho-sec*-phenethyl and strong electron-withdrawing *para*-fluorine groups of the ligand's aryl rings. Interestingly, the nickel *rac*-(*RS*)-**3b**/DEAC catalyst system could produce high stereoregularity of syndiotactic polystyrene at 70 °C due to its chiral bulky *sec*-phenethyl groups in the *ortho*-aryl position. The *pseudo*-square planar structure about the palladium center and poor leaving group, Cl, attached to palladium explains why *rac*-(*RR/SS*)-**3d** shows low catalytic activity for ethylene and styrene polymerization. Complex *rac*-(*RR/SS*)-**3d** also could produce syndiotactic polystyrene at 70 °C due to its chiral bulky *sec*-phenethyl groups in the *ortho*-aryl position.

Acknowledgments

We thank the National Natural Science Foundation of China (NSFC 21364011 and 20964003), the Scientific Research Foundation for the Returned Overseas Chinese Scholars of State Education Ministry (2009-1341), the Science and Technology Activities Merit-based Foundation for the Returned Overseas Chinese Scholars of State Human Resources and Social Security Ministry (2009-416) for funding. We also thank Key Laboratory of Eco-Environment-Related Polymer Materials of State Education Ministry, Key Laboratory of Polymer Materials of Gansu Province (Northwest Normal University), for financial support.

References

- [1] H. G. Alt, A. Koppl, *Chem. Rev.* **2000**, *100*, 1205.
[2] G. W. Coates, *Chem. Rev.* **2000**, *100*, 1223.
[3] E. Y.-X. Chen, T. J. Marks, *Chem. Rev.* **2000**, *100*, 1391.
[4] H. H. Brintzinger, D. Fischer, R. Mulhaupt, B. Rieger, R. Waymouth, *Angew. Chem. Int. Ed. Engl.* **1995**, *34*, 1143.
[5] Z. Zhang, Z. Ye, *Chem. Commun.* **2012**, *48*, 7940.
[6] G. Sun, J. Hentschel, Z. Guan, *ACS Macro. Lett.* **2012**, *1*, 585.
[7] C. S. Popeney, M. C. Lukowiak, C. Böttcher, B. Schade, P. Welker, D. Mangoldt, G. Gunkel, Z. Guan, R. Haag, *ACS Macro. Lett.* **2012**, *1*, 564.
[8] L. K. Johnson, C. M. Killian, M. Brookhart, *J. Am. Chem. Soc.* **1995**, *117*, 6414.
[9] H. Gao, H. Hu, F. Zhu, Q. Wu, *Chem. Commun.* **2012**, *48*, 3312.
[10] X. Shi, Y. Zhao, H. Gao, L. Zhang, F. Zhu, Q. Wu, *Macromol. Rapid Commun.* **2012**, *33*, 374.
[11] J. C. Yuan, T. J. Mei, P. T. Gomes, M. M. Marques, X. H. Wang, Y. F. Liu, C. P. Miao, X. L. Xie, *J. Organomet. Chem.* **2011**, *696*, 3251.
[12] J. C. Yuan, L. C. Silva, P. T. Gomes, J. M. Campos, M. R. Riberio, P. S. Valerga, J. C. W. Chien, M. M. Marques, *Polymer* **2005**, *46*, 2122.
[13] J. C. Yuan, F. Wang, W. Xu, T. Mei, J. Li, B. Yuan, F. Song, Z. Jia, *Organometallics* **2013**, *34*, 3960.
[14] D. H. Camachoa, Z. Guan, *Chem. Commun.* **2010**, *46*, 7879.
[15] Z. Guan, C. S. Popeney, *Top. Organomet. Chem.* **2009**, *26*, 179.
[16] C. Popeney, Z. Guan, *Organometallics* **2005**, *24*, 1145.
[17] S. D. Ittel, L. K. Johnson, M. Brookhart, *Chem. Rev.* **2000**, *100*, 1169.
[18] L. K. Johnson, S. Mecking, M. Brookhart, *J. Am. Chem. Soc.* **1996**, *118*, 267.
[19] S. Mecking, L. K. Johnson, L. Wang, M. Brookhart, *J. Am. Chem. Soc.* **1998**, *120*, 88.
[20] J. M. Rose, A. E. Cherian, G. W. Coates, *J. Am. Chem. Soc.* **2006**, *128*, 4186.
[21] A. E. Cherian, G. J. Domski, J. M. Rose, E. B. Lobkovsky, G. W. Coates, *Org. Lett.* **2005**, *7*, 5135.
[22] J. C. Yuan, F. Song, J. Li, Z. Jia, F. Wang, B. Yuan, *Inorg. Chim. Acta* **2013**, *400*, 99.
[23] F. Wang, J. C. Yuan, F. Song, J. Li, Z. Jia, B. Yuan, *Appl. Organomet. Chem.* **2013**, *27*, 319.
[24] J. C. Yuan, F. Wang, B. Yuan, Z. Jia, F. Song, J. Li, *J. Mol. Catal. A – Chem.* **2013**, *370*, 132.
[25] J. C. Yuan, Z. Jia, J. Li, F. Song, F. Wang, B. Yuan, *Trans. Metal Chem.* **2013**, *38*, 341.
[26] L. G. L. Ward, J. R. Pipal, *Inorg. Synth.* **1972**, *13*, 162.
[27] M. Brookhart, L. K. Johnson, C. M. Killian, S. D. Arthur, J. Feldman, E. F. McCord, S. J. McLain, K. A. Kreutzer, A. M. A. Bennett, E. B. Coughlin, S. D. Ittel, A. Parthasarathy, D. J. Tempel, WO Patent Application 9623010, 3 April, **1995**.
[28] a) Bruker, **2008**, APEX2, SAINT and SADABS. Bruker AXS Inc.: Madison, Wisconsin, USA; b) G. M. Sheldrick, SADABS-Bruker AXS area detector scaling and absorption, version 2008/1, University of Göttingen, Germany, **2008**.
[29] G. M. Sheldrick, *Acta Cryst.* **2008**, *A64*, 112.
[30] *CrysAlisPro 1.171.36.28*, Agilent Technologies Ltd.: Yarnton, Oxfordshire, UK, **2013**.
[31] L. Palatinus, S. J. Prathapa, S. Smaalen, *J. Appl. Cryst.* **2012**, *45*, 575.
[32] K. G. Van, K. Vrieze, *Adv. Organomet. Chem.* **1982**, *21*, 151.
[33] C. L. Song, L. M. Tang, Y. G. Li, X. F. Li, J. Chen, Y. S. Li, *J. Polym. Sci. Pol. Chem.* **2006**, *44*, 1964.
[34] R. J. Maldanis, J. S. Wood, A. Chandrasekaran, M. D. Rausch, J. C. W. Chien, *J. Organomet. Chem.* **2002**, *645*, 158.
[35] D. Meinhard, M. Wegner, G. Kipiani, A. Hearley, P. Reuter, S. Fischer, O. Marti, B. Rieger, *J. Am. Chem. Soc.* **2007**, *129*, 9182.
[36] G. B. Galland, R. F. Souza, R. S. Mauler, F. F. Nunes, *Macromolecules* **1999**, *32*, 1620.
[37] F. Feil, S. Harder, *Macromolecules* **2003**, *36*, 3446.
[38] L. Li, C. S. B. Gomes, P. S. Lopes, P. T. Gomes, H. P. Diogo, J. R. Ascenso, *Eur. Polym. J.* **2011**, *47*, 1636.
[39] Y. Li, M. Gao, Q. Wu, *Appl. Organometal. Chem.* **2008**, *22*, 659.
[40] F. Bao, R. Ma, X. Lu, G. Gui, Q. Wu, *Appl. Organometal. Chem.* **2006**, *20*, 32.

Supporting Information

Additional supporting information may be found in the online version of this article at the publisher's web-site.

CCDC 979684, 979688, 979687 and 979715 contain the supplementary crystallographic data for ligand **2b** and complexes **3a**, **3c** and **3d**. The data can be obtained free of charge via <http://www.ccdc.cam.ac.uk> or from the Cambridge Crystallographic Data Centre, 12 Union Road, Cambridge CB2 1EZ, UK; fax: (+44) 1223-336-033; or e-mail: deposit@ccdc.cam.ac.uk.